The Astrophysical Journal, 665:295–305, 2007 August 10

THE FORMATION OF GLOBULAR CLUSTER SYSTEMS IN MASSIVE ELLIPTICAL GALAXIES: GLOBULAR CLUSTER MULTIMODALITY FROM RADIAL VARIATION OF STELLAR POPULATIONS

Antonio Pipino,[1,2] Thomas H. Puzia,[3,4] and Francesca Matteucci[2]

Received 2006 December 20; accepted 2007 April 3

ABSTRACT

The most massive elliptical galaxies show a prominent multimodality in their globular cluster system color distributions. Understanding the mechanisms that lead to multiple globular cluster subpopulations is essential for a complete picture of massive-galaxy formation. By assuming that globular cluster formation traces the total star formation and taking into account the radial variations in the composite stellar populations predicted by the Pipino and Matteucci multizone photochemical evolution code, we compute the distribution of globular cluster properties as a function of galactocentric radius. We compare our results to the spectroscopic measurements of globular clusters in nearby early-type galaxies by Puzia and coworkers and show that the observed multimodality in globular cluster systems of massive ellipticals can be ascribed to the radial variation in the mix of stellar populations. Our model predicts the presence of a super-metal-rich population of globular clusters in the most massive elliptical galaxies, which is in very good agreement with the spectroscopic observations. The size of this high-metallicity population scales with galaxy mass, in the sense that more massive galaxies host larger such cluster populations. We predict an increase of mean metallicity of the globular cluster systems with host galaxy mass, and forecast that older clusters exhibit lower metallicities and higher α/Fe ratios. We find that a nonlinear color-metallicity relation may be partly responsible for a color multimodality. On the other hand, the formation of globular clusters from subsequently accreted gas, either with primordial abundances or solar metallicity, delivers model predictions that are at variance with the observations.

Subject headings: galaxies: elliptical and lenticular, cD — galaxies: formation — galaxies: star clusters — galaxies: structure — globular clusters: general

Online material: color figures

1. INTRODUCTION

1.1. *The Multimodality of Globular Cluster Systems*

One of the most significant developments in the study of extragalactic globular cluster systems (GCSs) was the discovery of bimodality in their color distributions (see Ashman & Zepf 1998; Harris 2001; West et al. 2004 and references therein). Today, we generally refer to globular clusters (GCs) belonging to the blue peak of the color distribution as metal-poor GCs and to the red-peak members as the metal-rich subpopulation. It is generally considered that the presence of multiple modes implies multiple distinct GC formation epochs and/or mechanisms and ties those directly into formation scenarios that have to describe the *parallel* assembly histories of GCSs *and* the diffuse stellar populations in their host galaxies. In massive early-type galaxies the current GCS assembly paradigms view the origin of the two color peaks from the perspective of either episodic star cluster formation bursts triggered by gas-rich galaxy mergers (e.g., Ashman & Zepf 1992), temporarily interrupted cluster formation (so-called in situ formation; e.g., Forbes et al. 1997; Harris et al. 1998), and star cluster accretion as a result of the hierarchical assembly of galaxies (e.g., Côté et al. 1998).

While the majority of GCSs in early-type galaxies show clearly bimodal color distributions, the general picture is much more complex, ranging from purely blue to purely red color distributions (e.g., Gebhardt & Kissler-Patig 1999; Kundu & Whitmore 2001a, 2001b; Larsen et al. 2001; Peng et al. 2006). This complexity is exacerbated by the fact that color bimodality is a function of galaxy mass and morphology, as less massive and later type galaxies tend to have single-mode blue (i.e., metal-poor) GC populations (e.g., Lotz et al. 2004; Sharina et al. 2005; Peng et al. 2006). Furthermore, color bimodality is also a function of galactocentric distance and is mainly due to the more extended spatial distribution of the metal-poor subpopulation relative to metal-rich clusters (e.g., Harris & Harris 2002; Rhode & Zepf 2004; Dirsch et al. 2003, 2005).

1.2. *Numerical Models of Globular Cluster System Formation*

The aspect of GCS formation and assembly entered recently the domain of numerical simulations of galaxy formation due to the increasing spatial resolution of these computations. For instance, Li et al. (2004) model GC formation by identifying absorbing sink particles in their smoothed particle hydrodynamics (SPH) high-resolution simulation of isolated gaseous disks and their mergers. They find a bimodal GC metallicity distribution in their merger remnant under the assumption of a particular age-metallicity relation. A key finding of their merger simulation is a more concentrated spatial distribution of metal-rich GCs with respect to the metal-poor subpopulation, in good agreement with observations. Since their models of isolated galaxies produce a smooth age distribution (implying a smooth metallicity and color distribution), Li et al. conclude that mergers are required to produce a bimodal metallicity (i.e., color) distribution.

In a more detailed adaptive-grid cosmological simulation, Kravtsov & Gnedin (2005) followed the formation of a star cluster system during the early evolution of a Milky Way–size

[1] Astrophysics, University of Oxford, Denys Wilkinson Building, Keble Road, Oxford OX1 3RH, UK; axp@astro.ox.ac.uk.

[2] Dipartimento di Astronomia, Università di Trieste, Via G. B. Tiepolo 11, 34100 Trieste, Italy; matteucci@ts.astro.it.

[3] Herzberg Institute of Astrophysics, 5071 West Saanich Road, Victoria, BC V9E 2E7, Canada; puziat@nrc.ca.

[4] Space Telescope Science Institute, 3700 San Martin Drive, Baltimore, MD 21218.

disk galaxy to redshift $z = 3$. Their model could reproduce the extended spatial distribution of metal-poor halo GCs as observed in M31 and the Milky Way. However, because their simulation does not follow the later evolution at $z < 3$ it is unclear whether it would produce a metallicity bimodality and any significant age-metallicity relation.

An alternative, more statistical approach to modeling GCS assembly is to directly link the mode of GC formation to the star formation rate in semianalytic models. Beasley et al. (2002) were the first to explore this path by assuming that metal-poor GCs form in gaseous protogalactic disks while metal-rich GCs are created during gaseous merger events. Their study showed that the observed GC color bimodality can only be reproduced by artificially stopping the formation of metal-poor GCs at redshifts $z \gtrsim 5$. By construction, no spatial information on metal-rich and/or metal-poor GCs is provided in these models.

1.3. *A Spatially Resolved Chemical Evolution Model for Spheroid Galaxies*

Recently, Pipino & Matteucci (2004, hereafter PM04) presented a spatially resolved chemical evolution model for the formation of spheroids, which successfully reproduces a large number of photochemical properties that could be inferred from either the optical or from the X-ray spectra of the light coming from ellipticals. The model includes an initial gas infall and a subsequent galactic wind; it takes into account detailed nucleosynthesis prescriptions of both Type II and Ia supernovae (SNe) as well as low- and intermediate-mass stars. It has been extensively tested against the main photochemical properties of nearby ellipticals, including the observed increase of the α-enhancement in their stellar populations with galaxy mass (e.g., Worthey et al. 1992; Weiss et al. 1995). This is at variance with standard models based on the hierarchical merging paradigm, which do not reproduce this trend (Thomas et al. 2002).

Since the PM04 model provides full radial information on the composite nature of stellar populations that make up elliptical galaxies, the observation of different GC subpopulations is, therefore, a new sanity check for the validity of this model. Moreover, we recall that PM04 and, more recently, Pipino et al. (2006, hereafter PMC06) suggested that elliptical galaxies should form outside-in; namely, the outermost regions form faster as well as develop an earlier galactic wind with respect to the central parts (see also Martinelli et al. 1998). This mechanism implies that the stars in massive spheroids form a composite stellar population (CSP), whose chemical properties, in particular their metallicity distribution, change with galactocentric distance.

Starting with the assumption that GC subpopulations trace the components of CSPs, we will show how the observed multimodality in GCSs can be ascribed to the radial variation in the underlying stellar populations. In particular, the observed GCSs are a linear combination of GC subpopulations inhabiting a given projected galactocentric radius.

The paper is organized as follows: in § 2 we briefly describe the adopted theoretical model; in § 3 we compare the predictions with observations and discuss the implications; and in § 4 we present our final conclusions.

2. THE MODEL

2.1. *The Chemical Evolution Code*

The chemical evolution code for elliptical galaxies adopted here is described in PM04, to which we refer the reader for more details. In the current work, we present the results for a galaxy with $M_{\rm lum} \sim 10^{11}\ M_{\odot}$, taken from PM04's model IIb. This model is characterized by a Salpeter (1955) IMF, Thielemann et al. (1996) yields for massive stars, Nomoto et al. (1997) yields for Type Ia SNe, and van den Hoek & Groenewegen (1997) yields for low- and intermediate-mass stars.

An important feature of the PM04 model is its multizone nature; namely, the model galaxy is divided into several noninteracting spherical shells of radius r_i, which facilitate a detailed study of the radial variation of the photochemical properties of the GCS and its host galaxy. In each zone i, the equations for the chemical evolution of 21 chemical elements are solved (see PM04; Matteucci 2001).

The model assumes that the galaxy is assembled by the merging of gaseous lumps on short timescales. The chemical composition of the lumps is assumed to be primordial. In fact, our model assumes that the accretion of primordial gas from the surroundings[5] is more efficient in more massive systems, given their higher cross section per unit mass (see PM04). The model galaxy suffers a strong starburst that injects a large amount of energy into the interstellar medium that is able to trigger a galactic wind, occurring at different times at different radii, mainly due to the radial variation of the potential well, which is shallower in the galactic outskirts. After the onset of wind activity the star formation is assumed to stop and the galaxy evolves passively with continuous mass loss. In order to correctly evaluate the amount of energy driving the wind, a detailed treatment of stellar feedback is included in the code (which takes into account the stellar lifetimes). In particular, the energy restored to the interstellar medium by both Type Ia and Type II SNe has been calculated in a self-consistent manner according to the time of explosion of each supernova and the characteristics of the ambient medium (see PM04 for details). The potential well that keeps the gas bound to the galaxy is assumed to be dominated by a diffuse and massive halo of dark matter surrounding the galaxy.

In the following we adopt the standard star formation rate $\psi_*(t,\ r_i) = \nu\, \rho_{\rm gas}(r_i,\ t)$ before the onset of the galactic wind ($t_{\rm gw}$), where $\rho_{\rm gas}$ is the gas density, ν the star formation efficiency; otherwise we assume that $\psi_*(t > t_{\rm gw},\ r_i) = 0$. We recall here that the adopted star formation efficiency is $\nu = 10\ {\rm Gyr}^{-1}$, while the infall timescale is $\tau = 0.4$ Gyr in the galactic core and $\tau = 0.01$ Gyr at one effective radius (of the diffuse light, $R_{\rm eff}$). These values were chosen by PM04 in order to reproduce the majority of the chemical and photometric properties of ellipticals such as the $[\langle {\rm Mg/Fe} \rangle]$-$\sigma$ (e.g., Faber et al. 1992), color-magnitude (e.g., Bower et al. 1992), and mass-metallicity relations (e.g., Gallazzi et al. 2005), as well as the observed gradients in metallicity (e.g., Carollo et al. 1993), $[\langle {\rm Mg/Fe} \rangle]$ (e.g., Mendez et al. 2005), and color (e.g., Peletier et al. 1990). Pipino et al. (2005) recently extended this model to explain also the properties of hot X-ray-emitting halos surrounding more massive spheroids.

2.2. *Globular Cluster Formation*

The formation rate of GCs, $\psi_{\rm GC}$, in the ith shell is assumed to be directly linked to its star formation rate $\psi_*(t,\ r_i,\ Z_i)$ via a suitable function of time t, radius r_i, and metallicity Z, which represents some scaling law between star formation rate ψ_* and the star cluster formation $\psi_{\rm GC}$ and can be regarded as a GC formation efficiency. A similar relation between the average star formation rate per surface area and the star cluster formation was recently found by Larsen & Richtler (2000) to hold in nearby spiral galaxies. In addition, the efficiency of cluster formation in massive ellipticals appears to be constant, where the mass ratio

[5] Since we lack a cosmological framework we cannot further specify the properties of the infalling primordial gas.

between the mass in star clusters and the baryons locked in field stars+gas is $\epsilon_{\rm GC} \approx 0.25\%$ (McLaughlin 1999). Here we extend this surface density relation to 3D space.

Moreover, PMC06 showed that at a given galactocentric radius model galaxies are made of a CSP, namely, a mixture of several simple stellar populations (SSPs), each with a single age and chemical composition. The CSP reflects the chemical enrichment history of the entire system, weighted by the star formation rate. We define the stellar metallicity distribution Υ_* as the distribution of stars belonging to a given CSP as a function of [Z/H].

We can then write the GC metallicity distribution $\Upsilon_{\rm GC}$ at a given radius r_i and time t as

$$\Upsilon_{\rm GC}(t,\ r_i,\ Z) = f(t,\ r_i,\ Z)\,\Upsilon_*(t,\ r_i,\ Z), \qquad (1)$$

where f includes all the information pertaining to the connection between $\psi_{\rm GC}$ and ψ_*.

It is not trivial, and beyond the scope of the paper, to find an explicit definition for $f(t,\ r_i,\ Z_i)$, which basically carries the information on the internal physics of gas clouds where GCs are expected to form. In the following we show that for a few and sensible choices of f, the observed multimodality in the color distribution of GCs may be driven by the radial variations in the stellar population mix of ellipticals. We first adopt a constant function f (see § 3.1) and then allow f to mildly vary with Z (see § 3.2). No absolute values for f are given, since our formalism deals with normalized distributions.

In particular, the *total* $\Upsilon_{\rm GC}$ summed over all radial shells can be written as

$$\Upsilon_{\rm GC,\,tot}(t,\ Z) = \sum_i f(t,\ r_i,\ Z)\,\Upsilon_*(t,\ r_i,\ Z). \qquad (2)$$

Similar equations hold for other GC distributions as a function of either [Mg/Fe] or [Fe/H].

At this stage it is useful to recall that $\Upsilon_*(t,\ r_i,\ Z)$ can be represented in two following ways: (1) as the fraction of mass of a CSP that is locked in stars at any given metallicity (Pagel & Patchett 1975; Matteucci 2001) (in the following we refer to this stellar metallicity distribution as $\Upsilon_{*,m}$, the mass-weighted stellar metallicity distribution); (2) as a fraction of luminosity of the CSP in each metallicity bin (this definition is closer to the measurement as it can be directly compared to the luminosity-weighted mean; $\Upsilon_{*,l}$ is the luminosity-weighted stellar metallicity distribution at a given radius; see Arimoto & Yoshii 1987; Gibson 1996). This classification is important since PMC06 showed that $\Upsilon_{*,m}$ and $\Upsilon_{*,l}$ might differ, especially at large radii, even for old stellar populations. The advantage of GCSs, for which accurate ages are known, is that they directly probe the mass-weighted distributions.

At this point it is useful to recall that our adopted chemical evolution model divides the galaxy into several noninteracting shells. In each shell the time at which the galactic wind occurs is self-consistently evaluated from the *local* condition. In particular, we follow the suggestion of Martinelli et al. (1998) that gradients can arise as a consequence of a more prolonged star formation period, and thus stronger chemical enrichment, in the inner zones. In the galactic core, in fact, the potential well is deeper and the supernova-driven wind develops later relative to the most external regions. This particular formation scenario leaves a characteristic imprint on the shape of both $\Upsilon_{*,m}$ and $\Upsilon_{*,l}$, and here we give some general considerations. In particular, we can explain the slow rise in the low-metallicity tail of the distributions as the effect of the initially infalling gas, whereas the onset of the galactic wind sets the maximum metallicity of $\Upsilon_{*,m}$ and $\Upsilon_{*,l}$. In general, the suggested outside-in formation process reflects in a more asymmetric stellar metallicity distribution at larger radii, where the galactic wind occurs earlier (i.e., closer to the peak of the star formation rate), with respect to the galactic center. The *qualitative* agreement between these model predictions and the observed stellar metallicity distributions derived at different radii by Harris & Harris (2002, see their Fig. 18) for the stars in the elliptical galaxy NGC 5128 is remarkable. If confirmed from observations in other ellipticals, the expected sharp truncation of $\Upsilon_{*,m}$ at large radii might be the first direct evidence of a sudden and strong wind that stopped the star formation earlier in the galactic outskirts (see PMC06; Pipino et al. 2007).

3. RESULTS AND DISCUSSION

3.1. *The Multimodality of Globular Cluster Systems in Elliptical Galaxies*

The general presence of multimodal GCSs implies that their host galaxies did not form in a single, isolated monolithic event, but experienced spatially and/or temporally separated star formation bursts. In the recent past, both semianalytic and hydrodynamic simulations of galaxy formation attempted to follow the process of GC formation (Beasley et al. 2002; Kravtsov & Gnedin 2005), but neither could produce a clearly bimodal metallicity distribution function (MDF) in their simulated GCSs.

In this section we show how to obtain a bimodal MDF for GCs $\Upsilon_{\rm GC,\,tot}$ starting from single-mode stellar MDFs $\Upsilon_*(t,\ r_i, Z)$ (commonly known as G dwarf–like diagrams) for the CSP inhabiting different radii of a prototypical elliptical galaxy according to equation (2).

3.1.1. *The Comparison Sample*

As stressed in the introduction, the multimodality in GCSs varies as a function of host galaxy properties (e.g., mass, morphological type). Here we try to match the distributions resulting from the recent compilation of spectroscopic data by Puzia et al. (2006, hereafter P06), which samples the typical bimodal color distribution of GCs in nearby galaxies (see also Puzia et al. 2004, 2005). This is illustrated in Figure 1, where we plot the $(V-I)_0$ color distribution of the P06 sample of GCs in elliptical galaxies (*top panel*), together with those of GCs in NGC 4472 and the Milky Way (*middle and bottom panels*). NGC 4472 is the most luminous elliptical in the Virgo galaxy cluster and hosts a GC system with a prototypical color bimodality (e.g., Puzia et al. 1999). To allow direct comparison with the P06 sample, we use GCs in NGC 4472 that are brighter than $V \simeq 22.5$ since the P06 sample includes only the brightest GCs in nearby early-type galaxies in order to maximize the S/N of their spectra. The resulting color distribution is remarkably similar to the one of the P06 sample, which assures that the P06 sample includes a representative sampling of the GC color bimodality in massive elliptical galaxies.

However, the comparison with the Milky Way GCs shows that the P06 sample covers few of the most metal-poor GCs. Therefore, the *bimodality* that we refer to in the following may not be the same as the one observed in spirals or in some elliptical galaxies, where a substantial population of metal-poor clusters with $[Z/{\rm H}] \lesssim -1.5$ is present (e.g., Gebhardt & Kissler-Patig 1999).

We do not include the dynamical evolution of GCs in our model, since we are considering only the brightest (most massive, i.e., $>10^{5.5}\,M_\odot$; see also Puzia et al. 2004) clusters in nearby galaxies as a comparison sample. The comparison sample includes GCs much brighter than the typical turnover magnitude of the GC luminosity function, and we therefore do not expect significant differential dynamical evolution for these massive

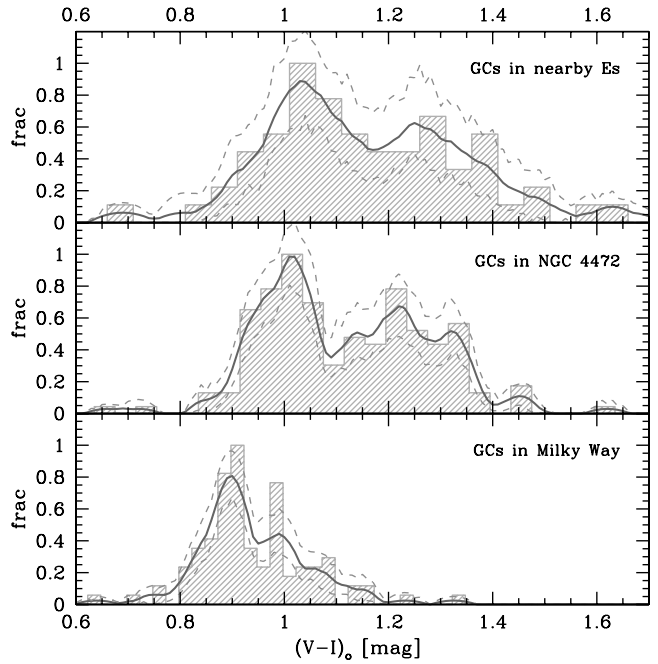

FIG. 1.—Color distributions of GCs in nearby, massive elliptical galaxies (Puzia et al. 2006; *top*), in NGC 4472 (Puzia et al. 1999; *middle*), and the Milky Way, taken from the 2003 February update of the McMaster catalog (Harris 1996; *bottom*). In order to allow a robust comparison between the P06 and NGC 4472 samples, only GCs in NGC 4472 with luminosities brighter than $V \simeq 22.5$ mag are shown. The solid lines are Epanechnikov-kernel probability density estimates with their bootstrapped 90% confidence limits. [*See the electronic edition of the Journal for a color version of this figure.*]

systems (see Gnedin & Ostriker 1997 for details). In fact, it has been shown (e.g., Fall & Zhang 2001) that the timescales for both evaporation by two-body relaxation and tidal stripping of star clusters is longer than a Hubble time for GCs more massive than $\sim 10^{5.5}\ M_\odot$.

In our model, the number of clusters formed in a star formation burst of a given strength is adjusted to match the observations. Hence, the absolute scaling of GC numbers is arbitrary; i.e., within the physical limitations of the star formation rate any number of GCs can be reproduced by adjusting the function f in equation (2).

If, however, metal-poor and metal-rich GCs are on systematically different orbits and experience significantly different dynamical evolutions, the effect of tidal disruption might be slowly changing relative GC numbers with time. Another complication is the variation of the initial star cluster mass function, in particular as a function of metallicity. Modeling these effects requires detailed knowledge of the orbital characteristics and chemodynamical processes that lead to star cluster formation, and goes far beyond the scope of this work. We keep these potential systematics in mind, but expect negligible impact on our analysis.

3.1.2. *A Simple Model*

In order to make a first-order comparison between our model predictions and the observed $\Upsilon_{\rm GC,\,tot}$ at $t = 13$ Gyr, we first focus on the simple case in which

$$\Upsilon_{\rm GC,\,tot}(Z) = f_{\rm red}\Upsilon_*(t = 13\ {\rm Gyr},\ r_1,\ Z) + f_{\rm blue}\Upsilon_*(t = 13\ {\rm Gyr},\ r_2,\ Z), \quad (3)$$

with $f_{\rm red}$, $f_{\rm blue} = {\rm const}$ and $r_1 = 0.1R_{\rm eff}$, $r_2 \geq 1R_{\rm eff}$. The first term (red) corresponds to a population typical of the galaxy core (well inside $r < 1R_{\rm eff}$). The second term (blue) represents Υ_* in the outer regions. In order to take into account the different amounts of stars formed in each galactic region, we point out that the stellar metallicity distributions entering equation (2) were not normalized.

As a first step, we take several values for the weights $f_{\rm red}$, $f_{\rm blue}$ in order to mimic different mixtures of the two GC populations. In particular, we used the relative numbers of the red (here identified as the metal-rich core population) and the blue GCs (the halo metal-poor population) as a function of galactocentric radius for the elliptical galaxy NGC 1399 (Dirsch et al. 2003). Our particular choice is driven by observationally motivated values for the weights, although we realize that NGC 1399 is a quite peculiar, massive cD elliptical and might not be representative of less massive systems. In the context of this first step, the weights might reflect the effects of the projection on the sky of a three-dimensional structure. However, we show below that the results do not strongly depend on the weights. Therefore they might be interpreted as mean values and could be changed if one decides to model a particular galaxy, with a different ellipticity, inclination, and luminosity profile.

In Figure 2 we show the GC metallicity distribution $\Upsilon_{\rm GC}$ by mass (computation based on $\Upsilon_{*,m}$) in two radial bins for three particular choices of weights. In particular, in the following we use the ratios $f_{\rm red} = 0.77, f_{\rm blue} = 0.23; f_{\rm red} = 0.60, f_{\rm blue} = 0.40$; and $f_{\rm red} = f_{\rm blue} = 0.50$ in order to define the theoretical innermost, intermediate, and outermost subsamples of the GCS, respectively. These $\Upsilon_{\rm GC}$ will be compared against subsamples of the P06 data, obtained by selecting GCs with either $r < 1R_{\rm eff}$ (in the case of the innermost population) or $r \geq 1R_{\rm eff}$ (for the intermediate and the outermost cases), unless otherwise stated.

3.1.3. *Globular Cluster Metallicity Distribution*

In order to plot the different cases on the same scale we normalize each $\Upsilon_{\rm GC}$ by its maximum value. In the left panel of Figure 2 the shaded histogram represents the innermost population. Our predictions match the data very well, especially in the metal-rich slope and the mean of the distribution. The same happens for the pure core populations, which shows how the GCS might be used to probe the CSP in ellipticals. It should be remarked that a second peak centered at supersolar metallicity, appears in the distribution predicted by our models, although not evident in the data of the particular radial subsample. The right panel of Figure 2 illustrates model predictions that are more representative of the galaxy as a whole (either at $1R_{\rm eff}$, i.e., the intermediate population, or at several effective radii, the outermost population), and we consider them as the fiducial case. These two cases look quite similar to each other and have clear signs of bimodality, in remarkable agreement with the spectroscopic data (*open histogram*; subsample of the P06 data with $r \geq R_{\rm eff}$). A Kolmogorov-Smirnov test returns >99% probability that both model predictions and observations are drawn from the same parent distribution in the left panel of Figure 2. The right panel statistics gives a lower likelihood of 98.4% that both distributions have the same origin, which is mainly due to the observed excess of metal-poor GCs at large galactocentric radii compared to the model predictions. The prediction of a supersolar metallicity GC subpopulation is entirely new and a result of the radially varying and violent formation of the parent galaxy. Moving to the low-metallicity tail, we predict slightly fewer low-metallicity objects than expected from observations. But we recall the systematics mentioned in § 3.1.1.

In Figure 3 (*left*) we show the results for a pure core GC, namely, one in which we adopt $f_{\rm red}$: $f_{\rm blue} = 1:0$. In this quite

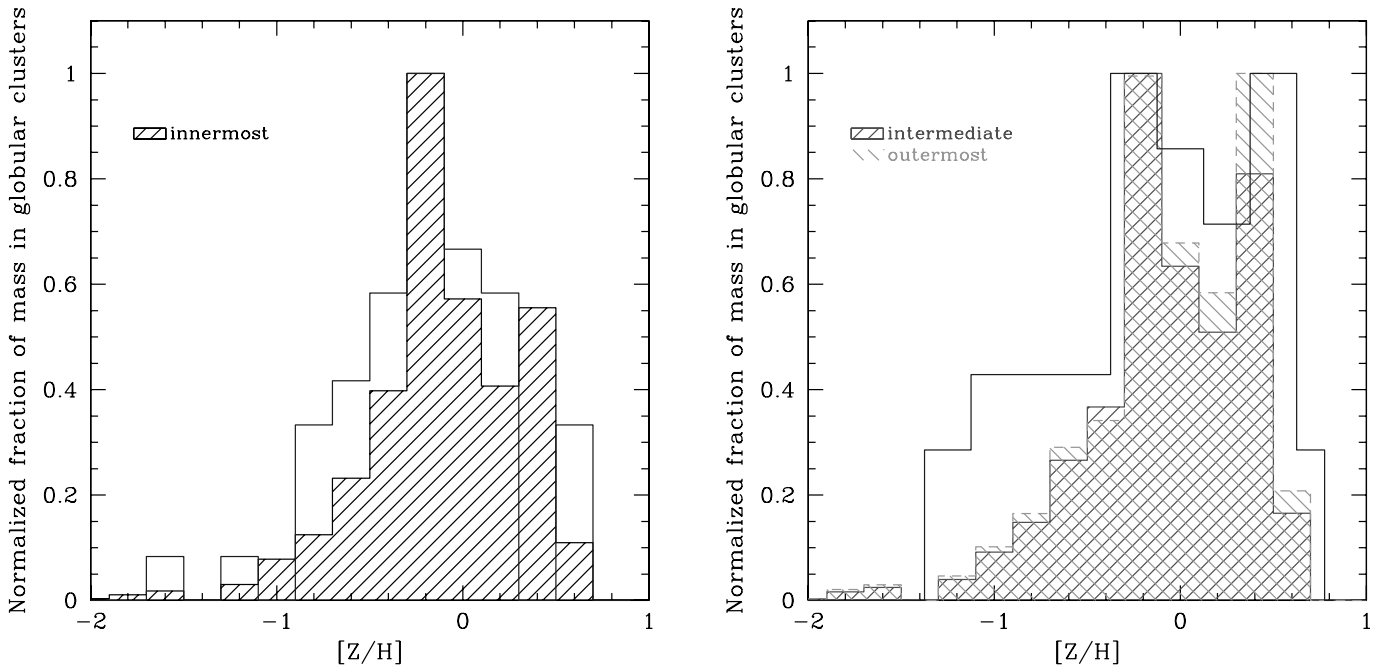

FIG. 2.—Predicted GC metallicity distribution $\Upsilon_{GC,tot}$ by mass as a function of $[Z/H]$ for three different radial compositions (i.e., f_{red}/f_{blue}). The left panel shows both model predictions and observations related to the central part of an elliptical galaxy. The right panel shows the same quantities for cluster populations residing at $r \geq R_{eff}$. *Open histograms*: Observational data taken as subsamples of the P06 compilation, according to the galactic regions presented in each panel. [*See the electronic edition of the Journal for a color version of this figure.*]

extreme case the observed GCs have been selected with radius $r < 0.5R_{eff}$. The histogram reflects the shape of a G dwarf–like diagram expected for a typical CSP inhabiting the galactic core. This finding is particularly important because it might offer the opportunity to resolve the SSPs in ellipticals, at variance with data coming from the integrated spectra, which deal with luminosity-weighted quantities. In Figure 3 (*right*) the intermediate population is compared to a subsample of P06 GCs with $0.5 < r < 0.5R_{eff}$. This is to show that the multimodality is not an artifact due to the particular radial binning adopted in this paper.

Figure 4 shows the V-band luminosity weighted Υ_{GC}, the computation for which is based on $\Upsilon_{*,l}$. This metallicity distribution has been obtained by converting the mass in each $[Z/H]$ bin of the previous figure into L_V, by means of the M/L_V ratio computed by Maraston (2005) as a function of $[Z/H]$ for 13 Gyr old SSPs. Due to the well-known increase of M/L_V in

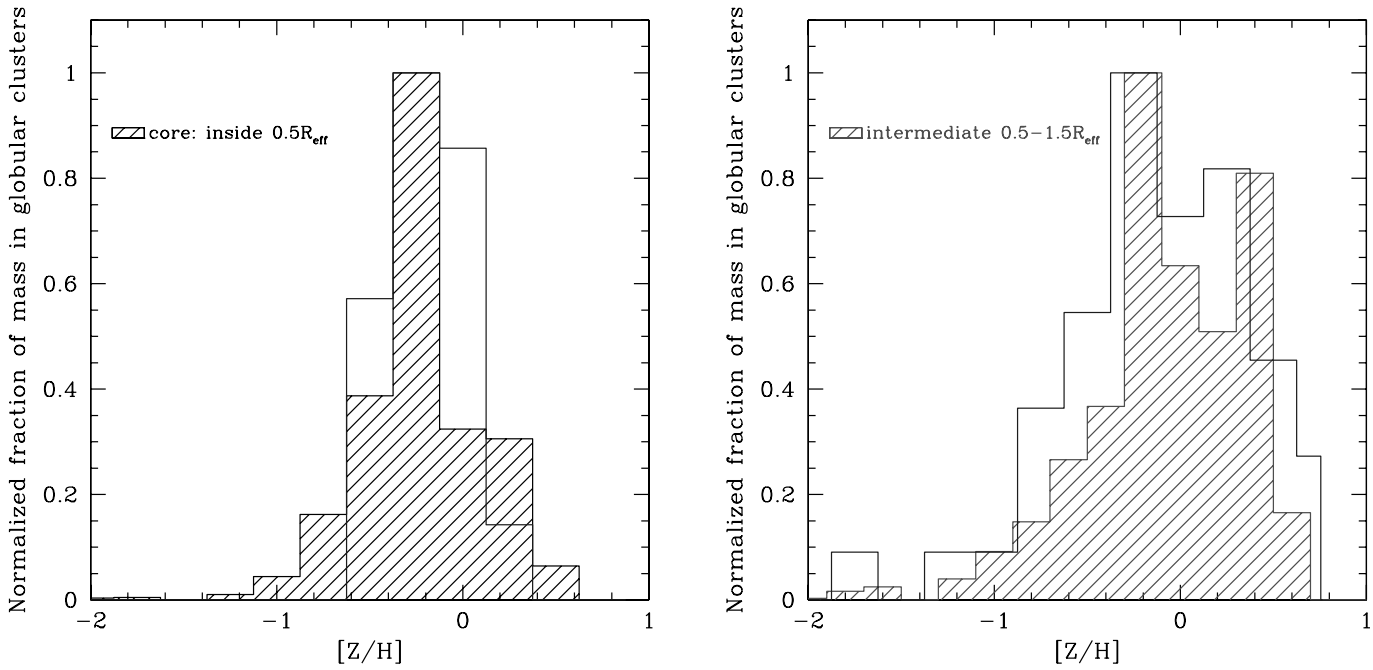

FIG. 3.—Predicted GC metallicity distribution $\Upsilon_{GC,tot}$ by mass as a function of $[Z/H]$ for two different projected galactocentric radii. The left panel shows both model predictions and observations related to the pure core of an elliptical galaxy (namely, $f_{red}:f_{blue} = 1:0$). The right panel shows the same quantities for cluster populations residing in the range $0.5R_{eff} < r < 1.5R_{eff}$. *Open histograms*: Observational data taken as subsamples of the P06 compilation, according to the galactic regions presented in each panel. [*See the electronic edition of the Journal for a color version of this figure.*]

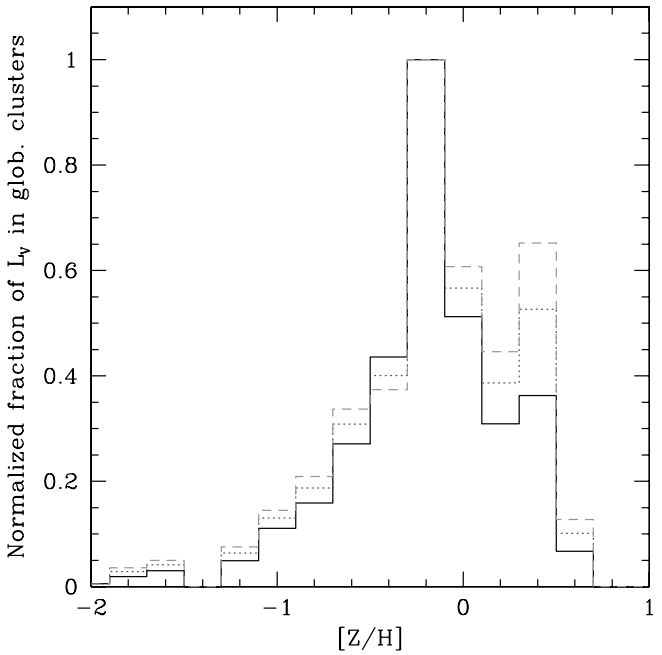

FIG. 4.—Predicted GC metallicity distribution $\Upsilon_{GC,tot}$ by luminosity at three different projected galactocentric radii. *Solid line*: Innermost region. *Dotted line*: Average galactic radius (intermediate population). *Dashed line*: Outermost part. [*See the electronic edition of the Journal for a color version of this figure.*]

the high-metallicity tail of the distribution,[6] we note in Figure 4 that now the second peak has a smaller intensity in all the cases. The corresponding diffuse-light population goes undetected in integrated-light studies. In any case, the conclusions reached by analyzing Figure 2 are not significantly altered. We conclude that our analysis is not significantly biased by some metallicity effect that may alter the shape of the observed $\Upsilon_{GC,tot}$ by luminosity. We stress the power of GCSs in disentangling stellar subpopulations in massive ellipticals, due to their nature as SSPs that can be directly compared to SSP model predictions, unlike diffuse-light measurements.

Even with this simple parameterization, where f in equation (3) does not depend on metallicity, we suggest that the bimodality for the metal-rich GCs is the result of different shapes of $\Upsilon_{*,m}$ (and $\Upsilon_{*,l}$) at different galactocentric radii.

3.1.4. *Globular Cluster* [Mg/Fe] *Distributions*

Finally, in Figure 5 we show the [Mg/Fe] distributions for GCs divided into radial bins as in Figure 2. According to PMC06, these [Mg/Fe] distributions are narrower, more symmetric, and exhibit a smaller radial variation with respect to the [Z/H] distributions. In any case, a small degree of bimodality is still present. We point out the impressive agreement with the spectroscopic observations by P06. There is a rather large discrepancy between data and models at the high-[Mg/Fe] end. Hence, the corresponding Kolmogorov-Smirnov likelihood tests return a probability of 1% (for inner sample) and 95% (for the outer ones). If we limit the model predictions to [Mg/Fe] < 0.8 dex, the agreement slightly improves, reaching a 10% probability in the inner region. However, the inner-field data still do not reach the extreme [Mg/Fe] values of the models. In fact, due to the monotonic decrease of the [Mg/Fe] as a function of either metallicity or time (see PM04), the lack of low-metallicity GCs, evident from Figure 2, translates into a lack of α-enhanced clusters.

The [Mg/Fe] bimodality of our model predictions and the match with the spectroscopic measurements strongly imply that GCs in massive elliptical galaxies form on two different timescales. Their chemical compositions are consistent with an *early* mode with a duration of $\Delta t \lesssim 100$ Myr and a *normal* formation that lasted for $\Delta t \lesssim 500$ Myr. In fact, according to the time-delay model (see Matteucci 2001) and given the typical star formation

[6] See PMC06 for a comparison between G dwarf–like diagrams for $\Upsilon_{*,m}$ and $\Upsilon_{*,l}$ predicted for the same CSP.

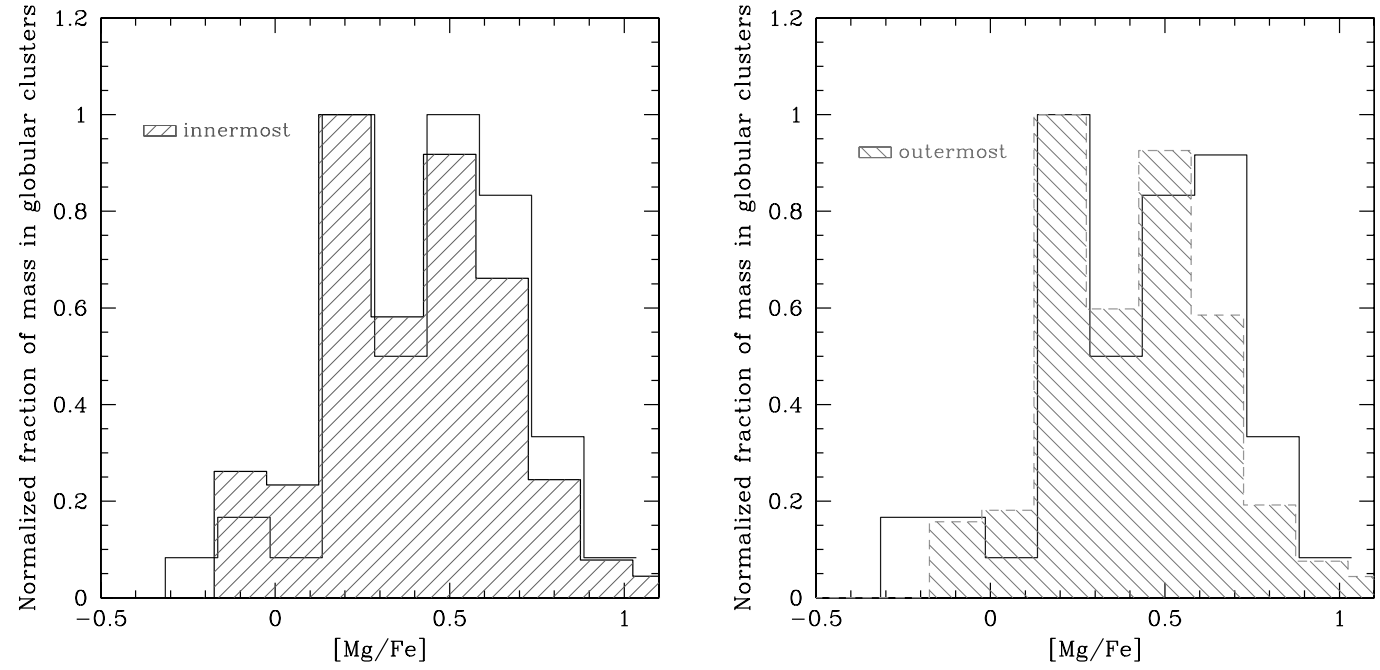

FIG. 5.—*Shaded histograms*: Predicted distribution of GC [Mg/Fe] values at two different projected galactocentric radii (innermost and outermost regions). *Open histograms*: Observational data taken as subsamples of the P06 compilation, according to the galactic regions presented in each panel (see text). [*See the electronic edition of the Journal for a color version of this figure.*]

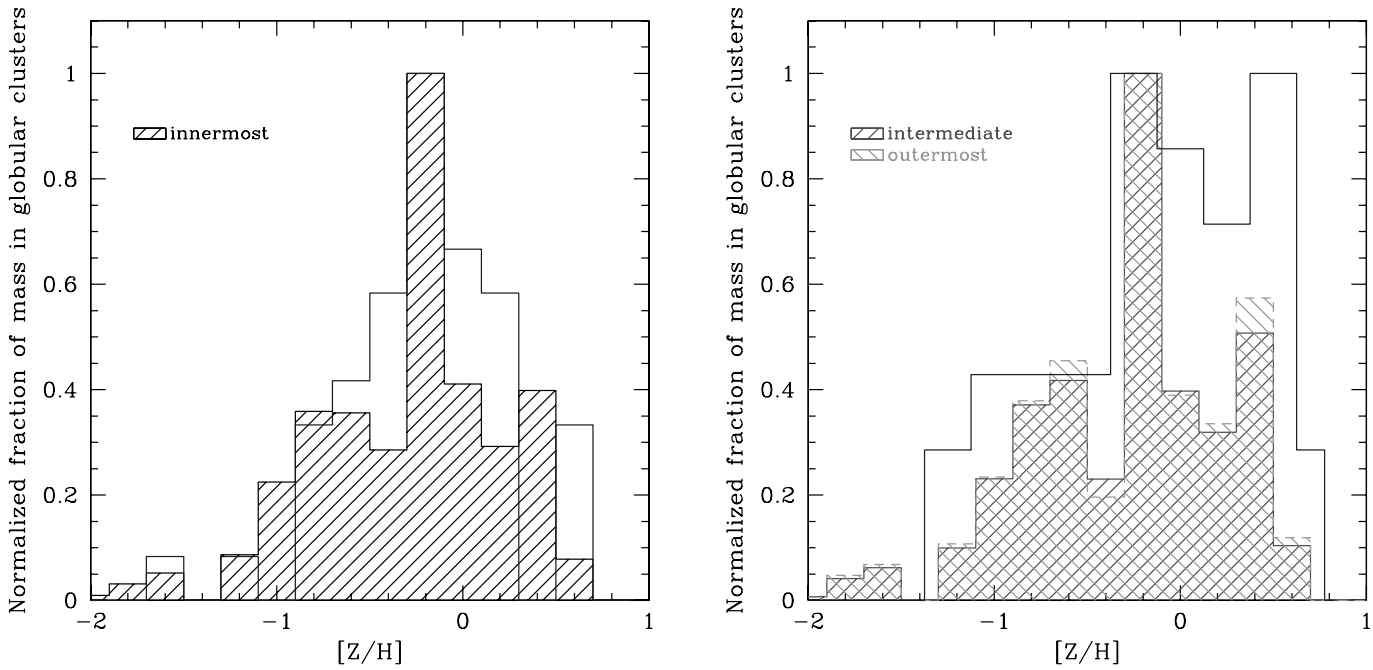

FIG. 6.—Predicted GC metallicity distribution $\Upsilon_{GC,tot}$ by mass as a function of $[Z/H]$ for three different radial compositions (i.e., different f_{red}/f_{blue}). In this case, the function f has an explicit dependence on $[Z/H]$ (see text). The left panel shows both model predictions and observations related to the central part of an elliptical galaxy. The right panel shows the same quantities for cluster populations residing at $r \geq R_{eff}$. *Open histograms*: Observational data taken as subsamples of the P06 compilation, according to the galactic regions presented in each panel. [*See the electronic edition of the Journal for a color version of this figure.*]

history of our model ellipticals, the [Mg/Fe] ratio in the gas—out of which the GCs form—is quickly and continuously decreasing with time. We predict that the [Mg/Fe] ratio can be higher than 0.65 dex (i.e., in the bins in which our predictions exhibit a deficit of GCs with respect to the observed distribution) only in the first ~100 Myr (see also Fig. 3 in P06 and related discussion). In fact, such a high value for the [Mg/Fe] can be attained only if very massive Type II SNe contribute to the chemical evolution, without any contribution from either lower mass Type II or Type Ia SNe. The normal formation, instead, is the one already plotted in Figure 5 and forms on a typical timescale of 0.5–0.7 Gyr. More quantitatively, our initial theoretical GC metallicity distribution predicts that only ~4% of the GCS forms at [Mg/Fe] larger than 0.65 dex. In order to improve the agreement with observations we require that the above fraction should be increased to ~12%–15%. Since star and GC formation are expected to be closely linked (e.g., Chandar et al. 2006), the same must be true for the diffuse stellar population of such galaxies. We therefore foresee the presence of a similar [Mg/Fe] bimodality in the diffuse light of massive elliptical galaxies. Unfortunately, we will not have direct observations confirming our suggestions until metallicity distributions for the diffuse stellar component in ellipticals become available for a number of galaxies. Indeed, the detection of bimodality in the [Mg/Fe] distribution might be a benchmark test for our predictions.

We will still refer to multiple GC subpopulations. However, their differences ought to be ascribed only to the fact that they are created during an extended (and intense) star formation event during which the variation in chemical evolution is not negligible. The radial differences originate from the fact that the galactic wind epoch is tightly linked to the potential, occurring later in the innermost regions (e.g., Carollo et al. 1993; Martinelli et al. 1998). Moreover, PM04 and PMC06 found that also the infall timescale is linked to the galactocentric radius. In particular, it lasts longer in the more internal regions, owing to the continuous gas flows in the center of the galactic potential well. In particular, we recall that in our model the core experiences a longer (~0.7 Gyr) star formation history with respect to the outskirts, where the typical star formation timescale is ~0.2 Gyr.

According to our models the metal-rich population of GCs in massive elliptical galaxies may consist of multiple subpopulations that basically play the same role as the CSPs populating each galactocentric shell in our framework of the global galaxy evolution. At the same time, we point out the failure of our models to produce a significant fraction of metal-poor GCs similar to the halo GC population in the Milky Way, with the caveat that the star formation histories are very different. This, in turn, suggests that GCSs in giant elliptical galaxies were assembled by accretion of a significant number of metal-poor GCs.

3.2. *Metallicity-dependent Globular Cluster Formation*

In this section we explore the approach outlined in equation (2), by introducing the effect of metallicity in the function f. In particular, we start by assuming that

$$\frac{f(t,\ r_i,\ [\mathrm{Z/H}] < -1)}{f(t,\ r_i,\ [\mathrm{Z/H}] > -1)} = 2, \tag{4}$$

roughly following what was found for the GCS of the most nearby giant elliptical galaxy, NGC 5128 (Centaurus A), by Harris & Harris (2002, hereafter HH02) for their "inner field," regardless of the radius of the ith shell. Since the final distributions are normalized, the actual zero point of the function f is not relevant. Our model predictions are plotted in Figure 6. We note a modest increase of the low-metallicity tail of the distribution with respect to the simple picture sketched in § 3.1 without metallicity dependence, as well as a lower fraction of GCs populating the high-metallicity peak. Including the metallicity dependence leads to an ambiguous change in agreement with the general observed trend. Hence, no firm conclusions on the real need for a metallicity dependence can be drawn. Similar results are obtained in the

more realistic case in which f is a linearly decreasing function of $[Z/H]$.

At variance with HH02, we chose to adopt the same scaling irrespective of galactocentric radius, for the following reason. Despite the fact that the HH02 stellar metallicity distributions Υ_* as functions of $[Z/H]$ confirm both the shape and the radial behavior of our model predictions for the mass-weighted stellar metallicity distribution $\Upsilon_{*,m}$ (compare their Fig. 7 with PMC06, Fig. 4), care should be taken when comparing their results for Υ_* as a function of [Fe/H]. The latter, in fact, had been obtained by assuming a particular trend in $[\alpha/\mathrm{Fe}]$ as a function of galactocentric radius that disagrees with the results of our detailed chemical evolution model. In particular, we find an offset of at least 0.2 dex in the sense that $[\mathrm{Fe/H}]_{\mathrm{HH02}} \sim 0.2 + [\mathrm{Fe/H}]_{\mathrm{PM04}}$ at a given metallicity ($[Z/H]$). This disagreement becomes larger either at very low metallicity or at larger galactocentric radii, where we expect a stronger α-enhancement. Once the PM04 value for [Fe/H] is adopted in Figure 18 of HH02, we find that (1) for the inner halo, the stellar $\Upsilon_{*,m}$ should be shifted by $\sim$0.2 dex toward lower metallicities, removing any metallicity effect, and (2) for the outer halo the discrepancy between the stellar $\Upsilon_{*,m}$ and the $\Upsilon_{\mathrm{GC,tot}}$ should be reduced.

Nevertheless, we believe that some decrease with time of the function f could be motivated by theoretical arguments. In fact, recent work (e.g., Elmegreen & Efremov 1997; Elmegreen 2004) shows that GCs of all ages preferentially form in turbulent high-pressure regions. If we interpret the decrease in the efficiency of star formation (inside the gas clouds that form GCs) as a function of the ambient pressure (Elmegreen & Efremov 1997) as a proxy for the temporal behavior of our function f, we find again a reduction of a factor $\sim$2–3 from the early high-pressure epochs to a late, more quiescent evolutionary phase.

3.2.1. *The Ratio of Metal-poor to Metal-rich Globular Clusters*

For our fiducial model we predict a ratio of metal-poor (namely, with $[Z/H] \leq -1$) to metal-rich GCs of $\sim$0.2. Previous photometric surveys found that the typical value for GC systems in elliptical galaxies is close to unity (Gebhardt & Kissler-Patig 1999; Kundu & Whitmore 2001a). Provided a linear color-metallicity transformation (see also § 3.5), a possible explanation for the discrepancy between our models and the observations might be obtained by boosting the metal-poor population by a factor of $f(t,\ r_i,\ [Z/H] < -1)/f(t,\ r_i,\ [Z/H] > -1) \geq 5$.

Another way to solve the discrepancy is to assume that all the *missing* GCs have been accreted from the surroundings, e.g., from dwarf satellites (e.g., Côté et al. 1998). We estimate the amount of the accreted metal-poor GCs needed to achieve a ratio close to 1 as a factor of $\sim$4 of the number of GCs initially formed inside the galaxy.

3.3. *The Role of the Host Galaxy Mass*

A natural consequence of the scenario depicted in §§ 3.1 and 3.2 is that at a given galactocentric radius, the mean metallicity and $[\alpha/\mathrm{Fe}]$ ratios of a GCS coincide with the mass-weighted $[\langle Z/\mathrm{H}\rangle_*]$ and $[\langle \alpha/\mathrm{Fe}\rangle_*]$ of the underlying stellar population, because the GC quantities are calculated either from $\Upsilon_{*,m}$ or $\Upsilon_{*,l}$ (see eqs. [1] and [2] of PMC06), unless the scaling function f is allowed to strongly vary with time. We expect this to happen at least in the innermost GC subpopulations, in which the effects of the accretion of GCs from the environment can be reasonably neglected. In particular, PM04 predict that more massive galaxies should show higher $[\langle \alpha/\mathrm{Fe}\rangle_*]$ and $[\langle Z/\mathrm{H}\rangle_*]$. If accretion plays a negligible role, we expect the same correlations for the *total* GC population with host galaxy mass for the most massive systems, in agreement with current observations (e.g., van den Bergh 1975; Brodie & Huchra 1991; Peng et al. 2006).

In fact, if we perform the same study of the above sections for a $10^{12}\ M_\odot$ galaxy (see Table 2 of PM04 for its properties), both peaks in $\Upsilon_{\mathrm{GC,tot}}$ shift their positions by about 0.2 dex to higher $[Z/H]$. This is in good agreement with the results of Peng et al. (2006; see their Figs. 13 and 14). This trend holds for smaller objects as well. If we apply the procedure to a $10^{10}\ M_\odot$ galaxy (model IIb of PM04), we find that the metal-rich peak shifts toward a lower metallicity by 0.3 dex (with respect to our fiducial model with $M_{\mathrm{lum}} = 10^{11}\ M_\odot$), while the other peak is now centered around $[Z/H] = -0.8$ dex. In particular, we find a faster decrease in the mean metallicity of the metal-poor GCs than for the metal-rich ones, again in agreement with the Peng et al. results.

Interestingly, the ratio of metal-poor to metal-rich clusters increases up to $\sim$0.5 for less massive halos. We recall that in the PM04 scenario, the low-mass galaxies are those forming on a longer timescale and with a slower infall rate. Therefore, we suggest that the combination of these factors is likely to at least partly explain the change of the GC distributions in different galaxy morphologies. This is especially the case in dwarf galaxies, where star formation is slow and still ongoing, together with the fact that the probability for a substantial change in the pressure of the interstellar medium relative to its initial values is higher than in ellipticals, thus implying a much stronger variation of f with time.

3.4. *Merger-induced Globular Cluster Formation*

It has been suggested that GC populations are produced during major merger events that would lead to present-day ellipticals and their rich GCSs (e.g., Schweizer 1987; Ashman & Zepf 1992). Subsequent studies (e.g., Forbes et al. 1997; Kissler-Patig et al. 1998b) challenged this view by pointing out the much higher S_N and more metal-rich GCSs in early-type galaxies compared to those of spiral and irregular galaxies, which are thought to represent the early building blocks of massive ellipticals.

In the following, we study the impact of the merger hypothesis on the predictions of our simulations. In order to do that, we extended the procedure sketched in the previous sections to the merger models presented by Pipino & Matteucci (2006, hereafter PM06). In that paper, the effects of late gas accretion episodes and subsequent merger-induced starbursts on the photochemical evolution of elliptical galaxies was studied and compared to the picture of galaxy formation emerging from PM04; in particular the PM04 best model was taken as a reference. By means of the comparison with the color-magnitude relations and the $[\langle \mathrm{Mg/Fe}\rangle_V]$-$\sigma$ relation observed in ellipticals (e.g., Renzini 2006), PM06 showed that both bursts involving a gas mass comparable to the mass already transformed into stars during the first episode of star formation and occurring at any redshift (major mergers), and bursts occurring at low redshift (i.e., $z \leq 0.2$) and with a large range of accreted mass (minor mergers), are ruled out. The reason lies in the fact that the chemical abundances in the ISM after the galactic wind (and before the occurrence of the merger) are dominated by Type Ia SN explosions, which continuously enrich the gas with their ejecta (mainly Fe). When the merger-induced starburst occurs, most stars form out of this enriched gas (thus, e.g., lowering the total $[\langle \mathrm{Mg/Fe}\rangle]$); at the same time, we expect the metallicities of GCs formed out of this gas to be on average higher and their [Mg/Fe] ratios to be lower than those of the bulk of stars and GCs formed in the initial starburst.

In this work we present the case in which the galaxy accretes a gas mass $M_{\mathrm{acc}} = M_{\mathrm{lum}}$ at $t_{\mathrm{acc}} = 2$ Gyr (i.e., $\sim$1 Gyr after the onset of the galactic wind). We make this choice for several reasons: (1) This model is quite similar to the PM06 models *b* and *g*,

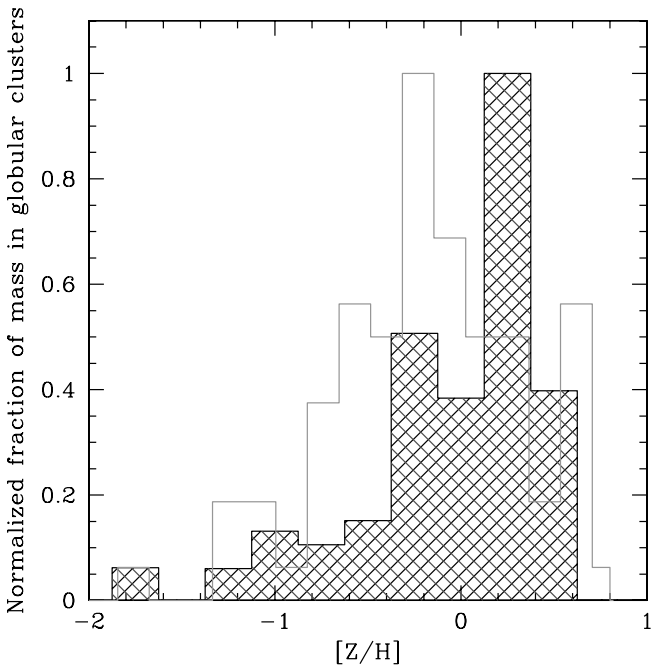

FIG. 7.—*Shaded histogram*: Predicted total GC metallicity distribution $\Upsilon_{\rm GC,tot}$ by mass for the $<1R_{\rm eff}$ shell, for a case in which a second episode of star formation, induced by a gaseous merger, is taken into account (see text). *Open histogram*: Observations from P06 (their entire sample). [*See the electronic edition of the Journal for a color version of this figure.*]

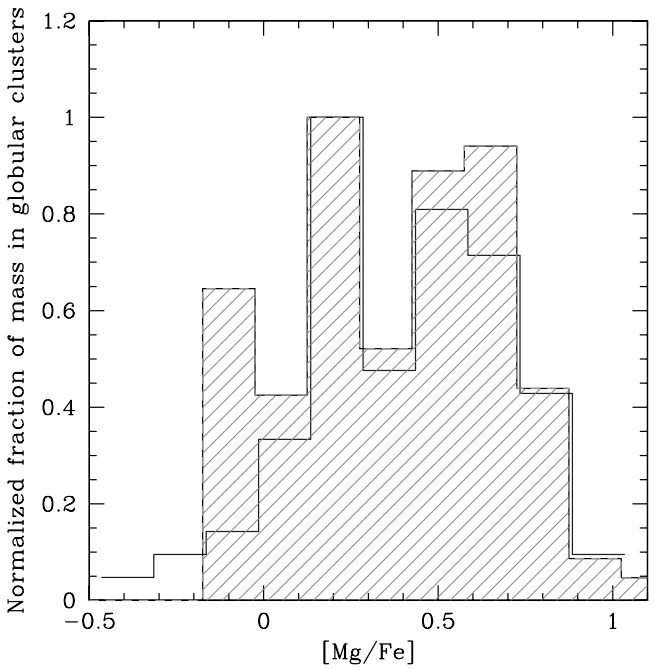

FIG. 8.—*Shaded histogram*: Predicted total GC [Mg/Fe] distribution by mass for the $<1R_{\rm eff}$ shell, for a case in which a second episode of star formation, induced by a gaseous merger, is taken into account (see text). *Open histogram*: Observations by P06 (their entire sample). [*See the electronic edition of the Journal for a color version of this figure.*]

which were among those in good agreement with observations of the diffuse galaxy light properties. (2) The formation epoch of the bulk of these second-generation GCs cannot occur $\gtrsim$2 Gyr later than $t_{\rm gw}$, because the majority of GCs in the most massive elliptical galaxies studied today appear old within the age resolution of current photometric ($\Delta t/t \approx 0.4$–0.5) and spectroscopic studies ($\Delta t/t \approx 0.2$–0.3). Finally, the composition of the newly accreted gas is assumed to be primordial (see PM06 for a detailed discussion), but we remark that we reach roughly the same conclusion in the case of solar composition, in order to mimic some preenrichment for the newly accreted gas. We point out that, lacking dynamics, PM06 presented their results for one-zone models. Therefore, in this section we are considering equation (2) limited to only one shell. In this way we can check whether the single merger hypothesis alone is enough to produce some bimodality in the total GC metallicity distribution $\Upsilon_{\rm GC,tot}$, and whether it is consistent with the predictions based on our fiducial model described in § 3.2.

We show our results in Figures 7 and 8. We note a clear change in the overall shape of the metallicity distribution $\Upsilon_{\rm GC,tot}$ with respect to the cases shown in the previous sections, in the sense that now $\Upsilon_{\rm GC,tot}$ is narrower and dominated by objects with supersolar metallicity (and subsolar [Mg/Fe] ratios) with a dominant population at $[Z/{\rm H}] \approx 0.1$, which is not prominent in the observations of P06. The high-metallicity GC populations dominate the metallicity distribution, which is at variance with both the results from previous sections and the observations.

Our merger model does not include the accretion of GCs that were already formed within the accreted satellite galaxies. The inclusion of this effect could remedy the match between models and observations at low metallicities, as the typical GC in a dwarf galaxy is metal-poor (e.g., Lotz et al. 2004; Sharina et al. 2005) and their addition to the initial GC population would enhance the total number of metal-poor GCs and improve the fit to the data. However, these clusters need to be α-enhanced to match the observations. The impact of GC accretion on our postmerger model predictions will be studied in detail in a future paper. Here we remark that the time at which the purely gaseous subsequent merger event can occur (which does not affect already formed GCs) is limited by the onset of the galactic wind, after which Type Ia SNe dominate the nucleosynthesis, and the fact that it must be completed at $t_{\rm mrg} \lesssim 1$–2 Gyr after the first starburst. However, this time constraint implies that such merger events would overlap with the initial starburst and be mostly indistinguishable from each other. Such a scenario closely resembles the Searle-Zinn scenario (Searle & Zinn 1978), in which galaxy halos are formed from the agglomeration of gaseous protogalactic fragments. Later merger events are excluded in our models, as they would produce GCs with subsolar [Mg/Fe] ratios, which is at variance with the observations.

Note also that the fraction of GCs at $[Z/{\rm H}] < -1$ can be recovered in our models only if the cluster formation at low metallicity is enhanced (e.g., using a value of 10 instead of 2 in eq. [4]). However, even in the case in which we adopt some $f(Z)$ strongly declining with total metallicity, which may alter the shape of $\Upsilon_{\rm GC,tot}$ enhancing the low-metallicity tail and thus improving the agreement with observations, the position of both supersolar metallicity peaks will not change, remaining at variance with the data.

3.5. *Other Mechanisms Responsible for Multimodality*

The picture emerging from our analysis is far from being the general solution to explaining the complexity of GC color distributions, and it suggests only a scheme in which multiple mechanisms could be at work together, either broadening or adding features to the observed distributions.

For instance, Yoon et al. (2006) suggested that the color bimodality could arise from the presence of hot horizontal-branch stars (so far not accounted for in SSP model predictions), which results in a nonlinear color-metallicity transformation producing

TABLE 1
NUMERICAL VALUES OF COEFFICIENTS USED IN EQUATION (5)

Coefficient	Numerical Value
α	1.5033
β	0.172774
γ	−0.623522
δ	−0.453331
ϵ	−0.089038

two color peaks from an originally single-peak metallicity distribution. We tested this scenario on our fiducial model GC metallicity distribution, by applying to each SSP the following transformation from [Fe/H] to the $(g-z)$ color:

$$(g-z) = \alpha + \beta[\mathrm{Fe/H}] + \gamma[\mathrm{Fe/H}]^2 + \delta[\mathrm{Fe/H}]^3 + \epsilon[\mathrm{Fe/H}]^4. \quad (5)$$

The numerical values of the coefficients are given in Table 1, and the relation was adopted from Yoon et al. (2006) and is consistent with the best-fit relation presented in their Figure 1*b*. We show our results in Figure 9.

Since we start from symmetric metallicity distributions, the nonlinear transformation seems to work and produce a color bimodality for the CSP inhabiting the $<10R_{\rm eff}$ shell (Fig. 9, *solid line*), although the bimodality is slightly exaggerated compared to real data (see Fig. 1). In fact, a look at the color distribution that we obtained for the sole $0.1R_{\rm eff}$ shell reveals that it still has one peak and is roughly symmetric (Fig. 9, *dashed line*). Obviously, since the $(g-z)$-[Fe/H] relationship is meant to explain the GCs' color bimodality without invoking any other effect, we did not combine the two histograms, either according to equation (2) or to equation (3) in our models, as we are comparing metallicity distributions to spectroscopic measurements.

It is of great importance to investigate this transformation with large and homogeneous data sets that cover a wide enough metallicity range to allow a robust analysis of the nonlinear inflection point in the color-metallicity transformation. However, as a result of Figure 9, we point out that the color bimodality typically found for GCSs in massive early-type galaxies might be only partly due to a nonlinear color-metallicity transformation.

Another effect put forward by, e.g., Recchi & Danziger (2005) is the claim that GCs might have undergone a self-enrichment phase at the early stages of their formation, and therefore some GCs could have experienced a boost in metallicity that would not be representative of the metallicity of their parent gas cloud. Finally, as already mentioned above in § 3.4, some GCs residing in the outermost regions of the galaxies (e.g., Lee et al. 2006) could have experienced entirely different chemical enrichment histories at the time of their formation and later been added to a more massive system through accretion (e.g., Côté et al. 1998). The inclusion of these effects goes far beyond the scope of this work, but we remind the reader that all the aforementioned effects might influence the interpretation of any GC color and metallicity distribution.

4. CONCLUSIONS

By means of the comparison between PM04's best model predictions for the radial changes in the CSP chemical properties and the recent spectroscopic data on the metallicity distributions of extragalactic GCSs from Puzia et al. (2006), we are able to derive some conclusions on the GC metallicity distributions in massive elliptical galaxies. In particular, we focused on the main drivers of the multimodality that is observed in the majority of GCSs in massive elliptical galaxies. Our main conclusions are as follows:

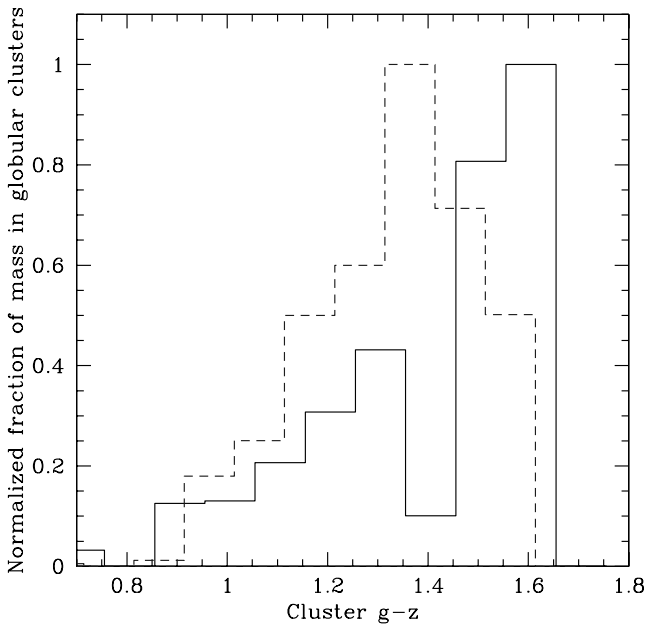

FIG. 9.—Predicted GC metallicity distribution by mass as a function of the $(g-z)$ color at two different projected galactocentric radii. *Dashed line*: Galactic core. *Solid line*: Galactic halo out to $10R_{\rm eff}$. [*See the electronic edition of the Journal for a color version of this figure.*]

1. We show that the observed multimodality in the GC metallicity distributions can be ascribed to the radial variation in the underlying stellar populations in giant elliptical galaxies. In particular, the observed GCSs are consistent with a linear combination of the GC subpopulations inhabiting different galactocentric radii projected on the sky.

2. A new prediction of our models, which is in astonishing agreement with the spectroscopic observations, is the presence of a supersolar metallicity mode that seems to emerge in the most massive elliptical galaxies. In smaller objects, this mode disappears quickly with decreasing stellar mass of the host galaxy.

3. Our models successfully reproduce the observed [Mg/Fe] bimodality in GCSs of massive elliptical galaxies. This, in turn, suggests a bimodality in formation timescales during the early formation epochs of GCs in massive galaxy halos. The two modes are consistent with an early (initial) and later (triggered) formation mode.

4. Since the GC populations trace the properties of galactic CSPs in our scenario, we predict an increase of the mean metallicity of the cluster system with the host galaxy mass, which closely follows the mass-metallicity relation for ellipticals. Moreover, we expect that a major fraction of the GCs (i.e., those born inside the galaxy) follow an age-metallicity relationship, in the sense that the older ones are also more α-enhanced and more metal-poor.

5. The role of host galaxy metallicity in shaping the observed GC metallicity distribution is nonnegligible, although its effects have been estimated to change the function $f \simeq \psi_{\rm GC}/\psi_*$ by a factor of $\sim$2–5, in order to match the sample of Puzia et al.

(2006). Either a nonlinear color-metallicity transformation, or a stronger metallicity effect, and/or accretion of GCs from the surrounding environment is needed to explain a ratio of metal-poor to metal-rich GCs close to unity, as reported for ellipticals based on results from photometric surveys.

6. Merger models that include the later accretion of primordial and/or solar-metallicity gas predict a shape for the GC metallicity distribution that is at variance with the spectroscopic observations.

We thank the referee for a careful reading of the paper. A. P. warmly thanks S. Recchi for useful discussions. A. P. acknowledges support by the Italian Ministry for University under the COFIN03 2003028039 scheme. T. H. P. acknowledges support by NASA through grants GO-10129 and GO-10515 from the Space Telescope Science Institute, which is operated by AURA, Inc., under NASA contract NAS5-26555, and support in the form of a Plaskett Research Fellowship at the Herzberg Institute of Astrophysics.

REFERENCES

Arimoto, N., & Yoshii, Y. 1987, A&A, 173, 23
Ashman, K. M., & Zepf, S. E. 1992, ApJ, 384, 50
———. 1998, Globular Cluster Systems, (Cambridge: Cambridge Univ. Press)
Beasley, M. A., Baugh, C. M., Forbes, D. A., Sharples, R. M., & Frenk, C. S. 2002, MNRAS, 333, 383
Bower, R. G., Lucey, J. R., & Ellis, R. S. 1992, MNRAS, 254, 601
Brodie, J. P., & Huchra, J. P. 1991, ApJ, 379, 157
Carollo, C. M., Danziger, I. J., & Buson, L. 1993, MNRAS, 265, 553
Chandar, R., Fall, S. M., & Whitmore, B. C. 2006, ApJ, 650, L111
Côté, P., Marzke, R. O., & West, M. J. 1998, ApJ, 501, 554
Dirsch, B., Richtler, T., Geisler, D., Forte, J. C., Bassino, L. P., & Gieren, W. P. 2003, AJ, 125, 1908
Dirsch, B., Schuberth, Y., & Richtler, T. 2005, A&A, 433, 43
Elmegreen, B. C. 2004, ASP Conf. Ser. 322, The Formation and Evolution of Massive Young Star Clusters, ed. H. J. G. L. M. Lamers, L. J. Smith, & A. Nota (San Francisco: ASP), 277
Elmegreen, B. G., & Efremov, Y. N. 1997, ApJ, 480, 235
Faber, S. M., Worthey, G., & Gonzalez, J. J. 1992, in IAU Symp. 149, The Stellar Populations of Galaxies, ed. B. Barbuy & A. Renzini (Dordrecht: Kluwer), 255
Fall, S. M., & Zhang, Q. 2001, ApJ, 561, 751
Forbes, D. A., Brodie, J. P., & Grillmair, C. J. 1997, AJ, 113, 1652
Gallazzi, A., Charlot, S., Brinchmann, J., White, S. D. M., & Tremonti, C. A. 2005, MNRAS, 362, 41
Gebhardt, K., & Kissler-Patig, M. 1999, AJ, 118, 1526
Gibson, B. K. 1996, MNRAS, 278, 829
Gnedin, O. Y., & Ostriker, J. P. 1997, ApJ, 474, 223
Harris, W. E. 1996, AJ, 112, 1487
———. 2001, in Star Clusters, ed. L. Labhardt & B. Binggeli (New York: Springer), 223
Harris, W. E., & Harris, G. L. H. 2002, AJ, 123, 3108 (HH02)
Harris, W. E., Harris, G. L. H., & McLaughlin, D. E. 1998, AJ, 115, 1801
Kissler-Patig, M., Forbes, D. A., & Minniti, D. 1998b, MNRAS, 298, 1123
Kravtsov, A. V., & Gnedin, O. Y. 2005, ApJ, 623, 650
Kundu, A., & Whitmore, B. C. 2001a, AJ, 121, 2950
———. 2001b, AJ, 122, 1251
Larsen, S. S., Brodie, J. P., Huchra, J. P., Forbes, D. A., & Grillmair, C. J. 2001, AJ, 121, 2974
Larsen, S. S., & Richtler, T. 2000, A&A, 354, 836
Lee, J.-W., López-Morales, M., & Carney, B. W. 2006, ApJ, 646, L119
Li, Y., Mac Low, M.-M., & Klessen, R. S. 2004, ApJ, 614, L29
Lotz, J. M., Miller, B. W., & Ferguson, H. C. 2004, ApJ, 613, 262
Maraston, C. 2005, MNRAS, 362, 799
Martinelli, A., Matteucci, F., & Colafrancesco, S. 1998, MNRAS, 298, 42
Matteucci, F. 2001, The Chemical Evolution of the Galaxy (Dordrecht: Kluwer)
McLaughlin, D. E. 1999, AJ, 117, 2398
Mendez, R. H., Thomas, D., Saglia, R. P., Maraston, C., Kudritzki, R. P., & Bender, R. 2005, ApJ, 627, 767
Nomoto, K., Iwamoto, K., Nakasato, N., Thielemann, F.-K., Brachwitz, F., Tsujimoto, T., Kubo, Y., & Kishimoto, N. 1997, Nucl. Phys. A, 621, 467
Pagel, B. E. J., & Patchett, B. E. 1975, MNRAS, 172, 13
Peletier, R. F., Davies, R. L., Illingworth, G. D., Davis, L. E., & Cawson, M. 1990, AJ, 100, 1091
Peng, E. W., et al. 2006, ApJ, 639, 95
Pipino, A., Kawata, D., Gibson, B. K., & Matteucci, F. 2005, A&A, 434, 553
Pipino, A., & Matteucci, F. 2004, MNRAS, 347, 968 (PM04)
———. 2006, MNRAS, 365, 1114 (PM06)
Pipino, A., Matteucci, F., & Chiappini, C. 2006, ApJ, 638, 739 (PMC06)
Pipino, A., et al. 2007, A&A, submitted (arXiv:0706.2932)
Puzia, T. H., Kissler-Patig, M., Brodie, J. P., & Huchra, J. P. 1999, AJ, 118, 2734
Puzia, T. H., Kissler-Patig, M., & Goudfrooij, P. 2006, ApJ, 648, 383 (P06)
Puzia, T. H., Kissler-Patig, M., Thomas, D., Maraston, C., Saglia, R. P., Bender, R., Goudfrooij, P., & Hempel, M. 2005, A&A, 439, 997
Puzia, T. H., et al. 2004, A&A, 415, 123
Recchi, S., & Danziger, I. J. 2005, A&A, 436, 145
Renzini, A. 2006, ARA&A, 44, 141
Rhode, K. L., & Zepf, S. E. 2004, AJ, 127, 302
Salpeter, E. E. 1955, ApJ, 121, 161
Schweizer, F. 1987, in Nearly Normal Galaxies (New York: Springer), 18
Searle, L., & Zinn, R. 1978, ApJ, 225, 357
Sharina, M. E., Puzia, T. H., & Makarov, D. I. 2005, A&A, 442, 85
Thielemann, F. K., Nomoto, K., & Hashimoto, M. 1996, ApJ, 460, 408
Thomas, D., Maraston, C., & Bender, R. 2002, Ap&SS, 281, 371
van den Bergh, S. 1975, ARA&A, 13, 217
van den Hoek, L. B., & Groenewegen, M. A. T. 1997, A&AS, 123, 305
Weiss, A., Peletier, R. F., & Matteucci, F. 1995, A&A, 296, 73
West, M. J., Côté, P., Marzke, R. O., & Jordán, A. 2004, Nature, 427, 31
Worthey, G., Faber, S. M., & Gonzalez, J. J. 1992, ApJ, 398, 69
Yoon, S.-J., Yi, S. K., & Lee, Y.-W. 2006, Science, 311, 1129